

# The 2019 Explosive Eruption of Raikoke Volcanic Island, Kuriles: Pyroclastic Deposits and Their Impact on the Relief and Ecosystems

S. Yu. Grishin<sup>a, \*</sup>, A. B. Belousov<sup>b, \*\*</sup>, M. G. Belousova<sup>b, \*\*</sup>, A. Auer<sup>c, \*\*\*</sup>, and I. A. Kozyrev<sup>b, \*\*</sup>

<sup>a</sup> Federal Center for Biodiversity Research, Far East Branch, Russian Academy of Sciences, prosp. 100 Years of Vladivostok, 159, Vladivostok, 690022 Russia

<sup>b</sup> Institute of Volcanology and Seismology, Far East Branch, Russian Academy of Sciences, bulv. Piipa, 9, Petropavlovsk-Kamchatsky, 683006 Russia

<sup>c</sup> Shimane University, Matsue, Japan, Yamashiro-cho 698-1, Matsue city, Shimane Prefecture, 690-0031 Japan

\*e-mail: grishin@biosoil.ru

\*\*e-mail: belousov@mail.ru

\*\*\*e-mail: auer@riko.shimane-u.ac.jp

Received December 11, 2020; revised February 16, 2021; accepted June 17, 2021

**Abstract**—A short-lived but violent explosive eruption occurred on the small volcanic island Raikoke in June 2019 (central Kuril Islands). The culmination of the eruption lasted 3.5 h and the ash cloud rose to a height of 13 km. An analysis of a sequence of satellite images in combination with ground-based observations gave information on the pyroclastic deposits of the eruption and allowed us to estimate the associated impact on the island ecosystems. We found that this eruption had a phreatomagmatic, sub-Plinian to Plinian character. The phreatomagmatic mechanism of the eruption occurred due to interaction between the rising basaltic andesite magma and ground waters, which were mostly represented by sea water that percolated through the permeable rocks of the volcanic island. The eruption produced numerous pyroclastic flows. The hot deposits of the pyroclastic flows and tephra covered the entire island, destroying the vegetation and the habitat of birds and sea mammals. Much of the pyroclasts was deposited in the form of fans of pyroclastic flows at the base of the volcanic slopes, considerably displacing the shoreline seaward. As a result, the island area increased by 15%. The pyroclastic deposits were intensely eroded and redeposited during the first year after the eruption, making new areas of the island coast. The recovery of Raikoke's ecosystems will be enhanced by erosion of the pyroclastic deposits and gradual resettling of birds, which would bring new plant species to the island. The succession would be accelerated by areas of survived vegetation. Overall, we see periodic dramatic disruptions in the island ecosystems caused by violent explosive eruptions with subsequent rapid recovery that with high probability will be interrupted by new eruption.

**Keywords:** Kuril Islands, Raikoke Island, eruption, pyroclastic deposits, ecosystems

**DOI:** 10.1134/S074204632105002X

## INTRODUCTION

Raikoke is a small (4.6 km<sup>2</sup> in area), uninhabited, and rarely visited volcanic island situated in the middle of the Kuril island arc 380 km southwest of Kamchatka (Figs. 1, 2).

The island never had permanent settlements, but in the past it was frequently visited by indigenous inhabitants (Ainu people) to hunt for birds and sea animals. The first description of Raikoke Volcano and its natural environment was made by the cossack commander Ivan Chernyi during his 1766–1769 expedition: "... the island has a big bare mountain from which stones were cast throughout the island; grass and roots are absent ...because the island has been thoroughly burned before" (quoted after (Polonsky, 1871, p. 429)). This description was interpreted by

G.S. Gorshkov (1954) to infer that a strong eruption occurred on the island in 1750–1760.

There were also strong explosive eruptions of the volcano in 1778 and in 1924. During the 1778 eruption 15 men were killed. In 1780, the cossack commander Sekerin who was sent to inspect the island after the eruption wrote a detailed description of the event: "During the large earthquake of 1778 accompanied by burning on the mount, its summit fell apart, and one third of the mountain collapsed, making heaps of rocks that covered the entire island and filled the bays. There was one more burning during the next night which caused part of the mountain to collapse, thus completing the destruction of the island. The debris killed the Cossack commander Chernyi with his comrades who temporarily camped there. The mountain was breached to the north, and its summit obtained a

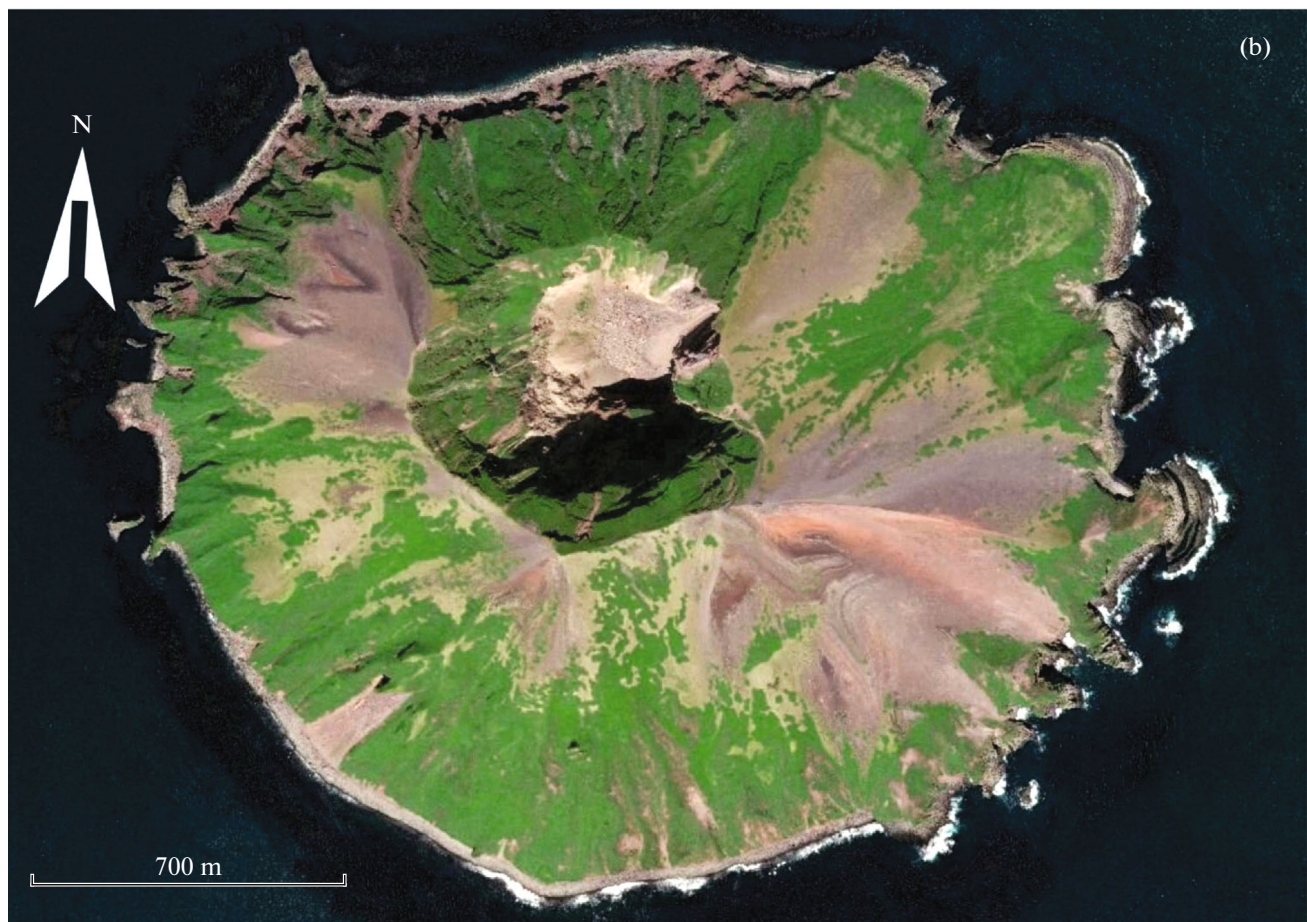
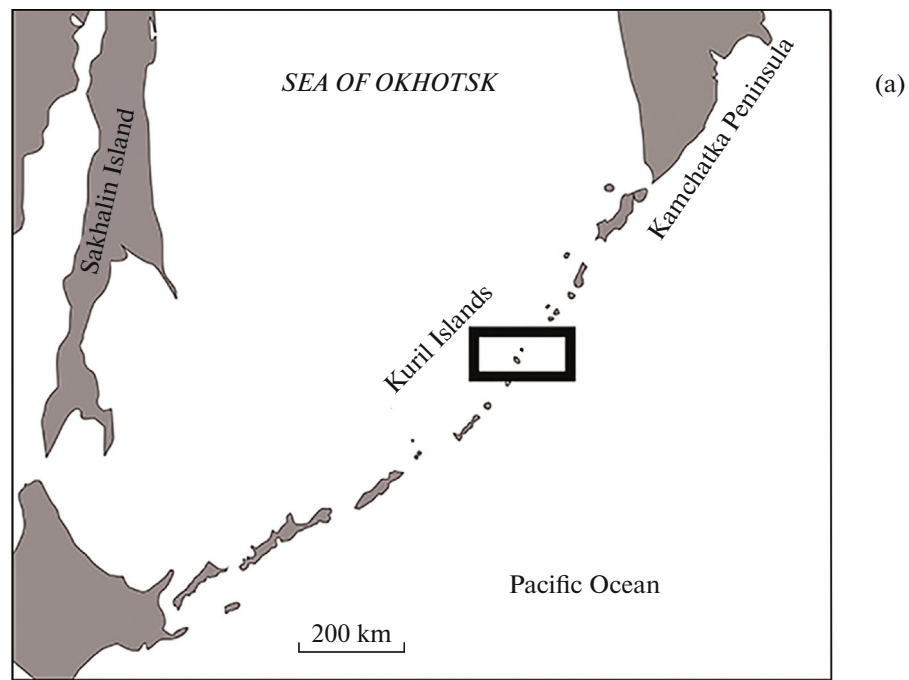


**Fig. 1.** The geographic position of Raikoke volcanic island. The rectangle shows the position of Raikoke Island (the north island) and that of Matua island (south of Raikoke) (a); Raikoke Island prior to the 2019 eruption on July 11, 2018 (the WorldView-2 satellite image) (b).

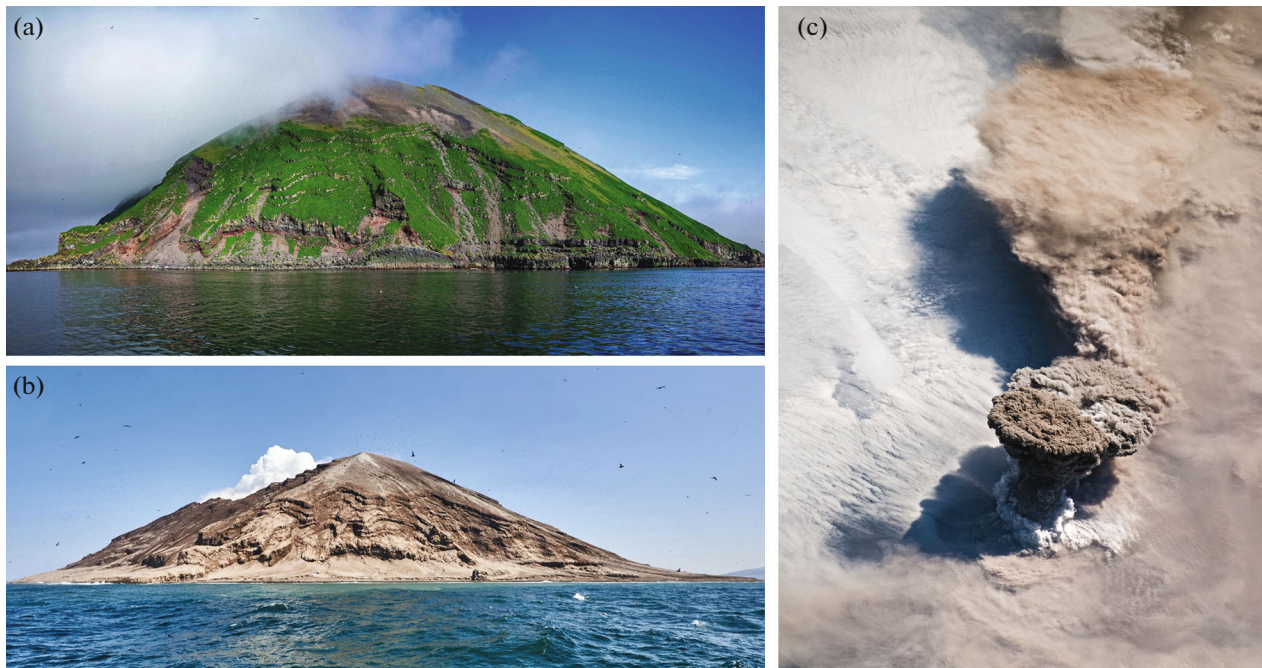


**Fig. 2.** View from northwest to Raikoke before the eruption (2016), as photographed by N.N. Pavlov (a) and after the eruption (September 2019), as photographed by E.V. Kaspersky (b). The eruption column during the beginning of the sub-Plinian phase on June 21, 2019 at 22:45 UTC; satellite image (<https://col.jsc.nasa.gov/SearchPhotos/photo.pl?mission=ISS059&roll=E&frame=119250>) (c).

shape of a saddle. Rocky sea cliffs were covered with sand and stones, making the place so smooth that birds had nowhere to breed; the boat harbour was filled with sand and the place became dryland; the nearshore shoal became a beach 200 m wide. The entire island was only covered with sand, while the mountain is making a terrible noise even now, but emits no smoke” (quoted after (Polonsky, 1871, pp. 429–430)).

Nearly 150 years later, on February 15, 1924, another eruption occurred. H. Tanakadate (1931) wrote: “A great cypressoid-like column of ash was noticed from the passing ship, the entire island was covered with fresh ash. Later on, a great quantity of white steam was emitted from the crater.” The crater of the volcano became much deeper (Gorshkov, 1958). This eruption was followed by a gradual recovery of the island’s ecosystem.

Volcanologists who saw the island in 1962 noted that it was sparsely vegetated on the slopes (Markhinin and Stratula, 1965).

The island biota was studied by an international expedition in 1996 and 2000 (Takahashi et al., 2002). Since the beginning of the 21st century there have been regular observations of the Steller sea lion rookery on the island (Trukhin, 2008; Burkanov et al., 2011). The volcano is not equipped with a ground network for instrumental monitoring, so that all information on its activity mostly comes from the analysis of satellite images. A short visit to the island in 2010

(Degterev and Chibisova, 2019) and our 2016 observations did not reveal any signs of volcanic activity. First observations of the eruption were conducted from the passing tourist vessel *Afina* during the terminal phase of the 2019 Raikoke eruption on June 23, 2019 (Fig. 3). Then after the eruption, Raikoke was briefly visited in July–September 2019 and in June–July 2020, when photographs and video surveys were made, including a video made from a drone which recorded the condition of natural environment on the island (N. Pavlov, E. Kaspersky, K. Burkard, and others).

The first reports on the eruption (Degterev and Chibisova, 2019; Girina et al., 2019; Rashidov et al., 2019) contain few information on the pyroclastic deposits and their impact on Raikoke’s natural environment. The scale of the eruption’s impact and the dynamics of transformations affecting the deposits after the eruption were determined by us through comparisons between the satellite images taken before and after the eruption, as well as during the 2020 expedition to the island.

## METHODOLOGY

The dynamics of the transformations that affected the deposits after the eruption was made clear by comparing the series of images from Sentinel-2, Landsat 8, and WorldView-1, 2 satellites during the period from June 2019 to September 2020 and during the period before the eruption since 1972. The satellite images

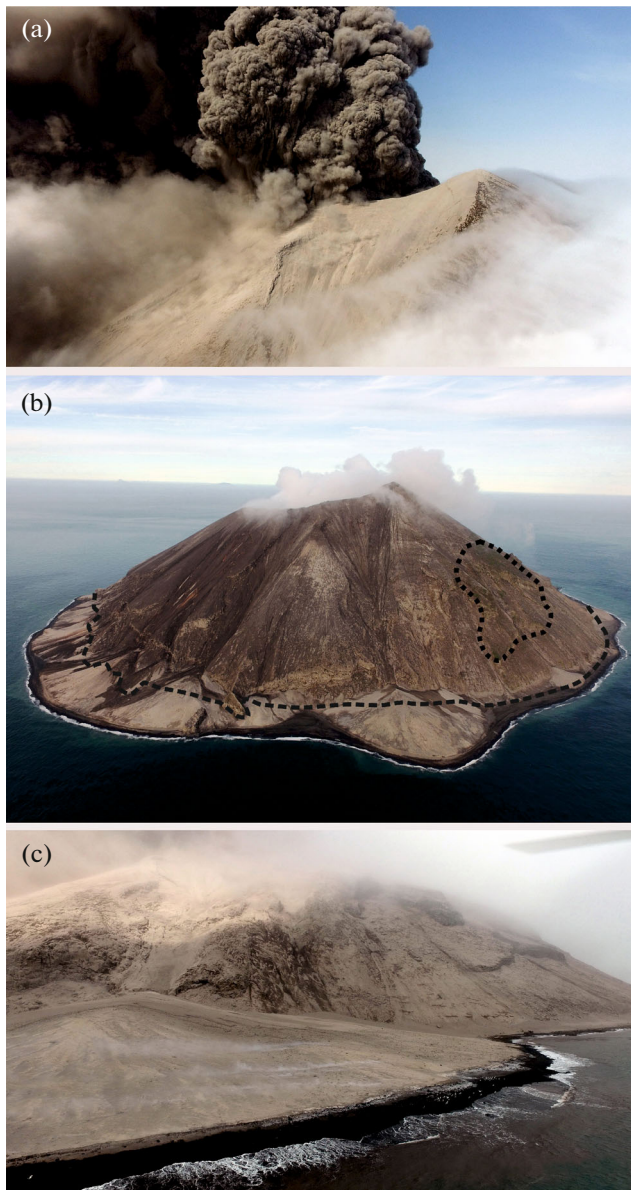


**Fig. 3.** The ash plume in the crater area of Raikoke volcanic island, during the terminal phase on June 23, 2019 at 17:45 (a). A general view of the island: on the northwestern coast there is a new coastline, in the southwestern coast—a large fan of pyroclastic deposits. The intermittent line shows the coastline prior to the 2019 eruption, the dotted line encloses the area with fragments of surviving vegetation on the slope, September 8, 2019 (b). The fan consisting of hot pyroclastic flow deposits on the southwestern coast, June 23, 2019 (c). Photographed by N.N. Pavlov.

studied by us have low resolution, so the resulting quantitative estimates are rather approximate.

A field survey and sampling of the pyroclastic deposits of the 2019 eruption were carried out in July 2020 on the eastern coast of the island. We did a grain-size analysis of samples taken from pyroclastic flows using the standard method of dry sieving (Walker,

1971). The density and vesicularity of juvenile basaltic andesite were determined for four rock samples 2–3 cm across by the method based on Archimedes' principle of buoyancy using the difference between the sample weights in distilled water and air (Hoblitt and Harmon, 1993). Before we weighed the samples in water we covered them with waterproof spray containing silicon oil; afterwards, the samples were dried in a furnace during 24 hours at a temperature of 60°C. The vesicularity index (Houghton and Wilson, 1989) was determined using the density of non-vesicular low-silica andesite 2.7 g/cm<sup>3</sup>.

We determined the chemical composition of juvenile material for the 2019 eruption using a JEOL 8530F microprobe and a RIX-2000 spectrometer (Faculty of Geosciences, Shimane University, Japan).

### RAIKOKE ISLAND BEFORE THE 2019 ERUPTION

Raikoke island, 551 m a.s.l. high, is the upper part of the cone of an active stratovolcano whose base is at 2500 m depth on the bottom of the eastern margin of the Sea of Okhotsk (Gorshkov, 1967) (see Fig. 2a). The volcano has steep (30° and more) and short slopes (the distance from the crater rim to the shore is 400–1000 m in map view). The slopes are complicated in many locations by steplike escarpments up to 5 m, which expose a layered sequence of lava flows of “aa” type. The thick frontal parts of the flows step out 100–200 m into the sea. There are landslides in the lower parts of the slopes, with the largest being about 300 m long and up to 100 m wide.

There had been extensive taluses of pyroclastic material on the volcano slopes prior to the eruption. Some of these were up to 1000 m long and extended from the crater rim to the shoreline (see Fig. 1b). There was a deep (over 400 m) crater 700–750 m across at the summit of the volcanic cone in the middle of the island; the northern part of the crater rim is 220 m lower than its southern part. The crater has the steep inner slopes and the bottom covered by large blocks and pebble taluses with the area about 0.15 km<sup>2</sup> (see Fig. 1b).

The condition of the biota on the island as of 2019 was in agreement with the relatively short (95 years) period of incomplete recovery following the catastrophic impact of the 1924 eruption. The available satellite image (Landsat, 1972) of the island shows the patches of barren land and green patches covered by vegetation, their distribution in general corresponded with the distribution of vegetation before the 2019 eruption. According to the data acquired in 1996 and 2000, on the island was found 68 species of vascular plants (Takahashi et al., 2002). The meadow and shrub vegetation prevailed. It had covered at least 60% of the volcano's outer slopes and ~70% of the inner slopes by 2018 (see Fig. 1b). Closed vegetation was observed at

the base of the volcanic cone and on the northward slopes where it was formed on bedrock exposures of older lava flows. The extensive barren lands and taluses in the lower slopes began to form a moss cover as reported by V.Yu. Barkalov (personal communication). The upper slopes were extensive barren lands that were either poorly covered by plants or not at all. One important special feature of the island's ecosystems were consisted in a great number of nesting birds (about 260000); these comprised 15–16 species, including the largest (in the northern Pacific) breeding site of the Northern Fulmar (*Fulmarus glacialis*) (Trukhin, 2008). During periods between eruptions, some small amounts of volcanic ash was transported to the island from other volcanoes of the Kuril island arc. Part of the environment that surrounded the island along the coast were algae thickets in the coastal strip 25 to 350 m wide: the strip was the narrowest in areas adjacent to the lava capes in the northeastern island area, and very wide, with dense thickets, in the southern shore. The coast of the western part of the island had a breeding site of Steller sea lions (*Eumetopias jubatus*) where much of the Kuril population of that species was concentrated. Their counting in 2018 estimated 474 individual animals, including 138 cubs (Burkanov et al., 2020).

#### THE 2019 ERUPTION AND ITS IMPACT

The timing of the eruption was reconstructed by Degterev and Chibisova (2019) based on an analysis of satellite images, as well as by Firstov et al. (2020) by an analysis of acoustic signals connected with the eruption.

The eruption started at about 18:00 UTC on June 21, 2019 (June 22 at 5:00 local Sakhalin time). The initial phase of the eruption (discrete outbursts) lasted 4.5 hours and consisted of 6 ash outbursts lasting 20 to 40 min each, ejecting ash to heights up to 10 km a.s.l. At 22:30 UTC the culminating phase began (a Plinian phase of continuous pyroclastic discharge), with the ash plume rising to a height of 13 km (see Fig. 2c).

**The 2019 deposits.** The small area of the island and its slope steepness do not favor the accumulation and preservation of Raikoke pyroclastic deposits. The pyroclastic flow deposits were studied at outcrops in the small (3–8 m high) coastal cliffs eroded by the sea. Maximum thickness of the deposits is up to 10–15 m. By the time the study began, in July 2020, the deposits were completely cooled down. The studied outcrops show that the fans consist of numerous (3 to 5) units of pyroclastic flows, each being 1 to 3 m thick (Fig. 4a). The boundaries between successive flow units are well defined, but the contacts between them are not sharp and more frequently gradual, which is the evidence of a quick deposition without considerable time interval. Flow units mostly differ by concentration and, to a lesser extent, by the grain size of coarse material in their composition (see Fig. 4b). The pyroclastic flow

deposits are poorly sorted (sorting is 2–3  $\phi$ ) (Inman, 1952), grey sandy gravel with admixture of larger rock fragments up to 10–20 cm across, occasionally reaching 50 cm. The fraction of the gravel is 35–70%, that of the sand is 30–60% (Fig. 5). The deposits of pyroclastic flows are notably compacted and not cemented. Signs of intensive degassing of the deposits have not been found, although photographs made immediately after the eruption show some steam fumaroles on the surface of fresh flows (see Fig. 3c).

The clastic material in the flows has a variable petrographic composition. The rock fragments are mostly non-juvenile, lithic and angular. Some of them are oxidized and are hydrothermally altered. Part of this clastic material was ejected by the eruption, and another part was eroded by pyroclastic flows from the volcano's slopes. Visual inspection allowed to distinguish 3 types of juvenile material: dark-grey scoriaceous, grey scoriaceous and light grey pumiceous basaltic andesites. Chemical analyses are shown in Fig. 6, Table 1. The juvenile material has a density of 1.63–1.81 g/cm<sup>3</sup>, the vesicularity index is 33–40%. Also some pyroclastic flows contain rounded, very dense fragments of various olivine-bearing, macro-crystalline rocks like cumulates/allivalites up to 5–10 cm across.

Higher on the steep slopes (outside the fans) the pyroclastic deposits of the last eruption are thin (20–30 cm or less) or entirely absent, and the pre-eruption soil (substrate of the pyroclastic deposits) is scoured and smoothed out. The remains of plant do not have obvious signs of charring; that means that the pyroclastic flows had moderate temperatures, probably not higher than 200–300°C. The pyroclastic flow deposits in some places are covered by the lenticular deposits of coarse Plinian tephra: unconsolidated friable lapilli (2–5 cm across) and bombs (up to 20–30 cm) of dark-grey scoriaceous basaltic andesite (see Fig. 4c, Table 1).

**Reconstructing the dynamics and the mechanism of the eruption.** Comparison of the timing of the 2019 eruption (Degterev and Chibisova, 2019; Firstov et al., 2020) with characteristics of the studied pyroclastic deposits allow us to suggest the following sequence of events of the 2019 eruption. The eruption started abruptly and immediately reached high explosivity. The high rate of magma ascent is indicated by the presence of dense cumulates in the pyroclastic flow deposits; this is typical for strong explosive eruptions (Plechov et al., 2008).

The initial phase of the eruption (that of discrete volcanic outbursts after Degterev and Chibisova (2019)) lasting from 18:00 to 22:30 UTC June 21, 2019 was probably phreatomagmatic and sub-Plinian in character. The pulsating eruption column that occasionally rose to 10 km height was overcharged with fine-grained pyroclastic material and frequently collapsed, producing numerous small pyroclastic flows that were moving in radial directions from the crater over all slopes toward the sea shore, and went farther

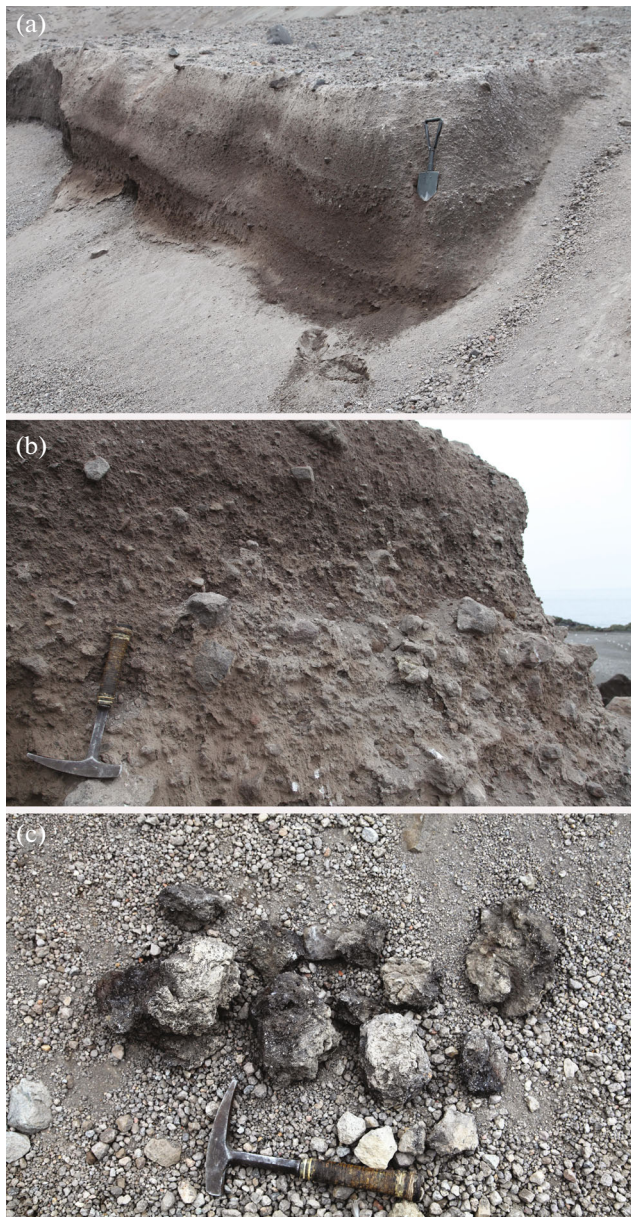


**Fig. 4.** The pyroclastic deposits of the 2019 eruption of Raikoke volcano. A cross section of pyroclastic flow deposits consisting of three layers or units that resulted from the collapse of the eruption column of 2019 phreatomagmatic sub-Plinian eruption (a). The contact of two units of pyroclastic flows with different concentration and grain size of coarse-grained material (b). Lapilli and bombs of scoriaceous basaltic andesite of the magmatic (Plinian) phase of the 2019 eruption (c). Photographed by A.B. Belousov.

into the sea for some distance. The flows descended along the preexisting erosion gullies on the volcanic slopes, emplacing pyroclastic fans at the outlets of gullies (see Figs. 3b, 3c). During the eruption course, the amount of ground water contacting with magma decreased (or stopped), and for a short time (3.5 h)

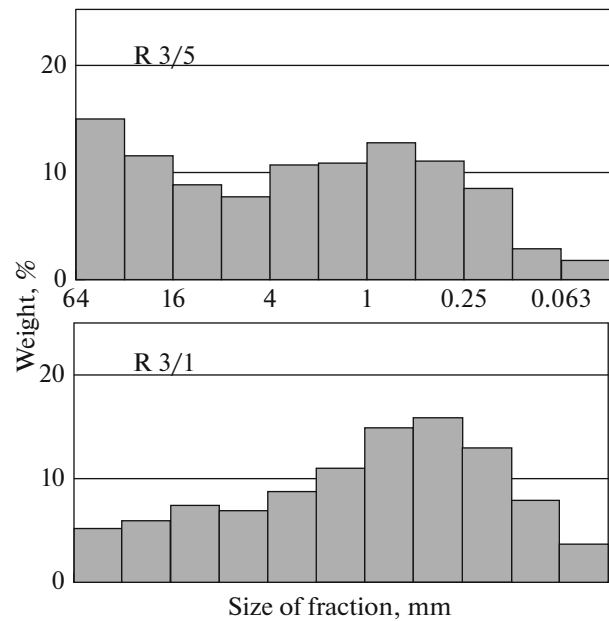


**Fig. 5.** Histograms showing the grain-size composition for two units of pyroclastic flow (3/1 lower unit, 3/5 upper unit).

the fragmentation of magma became purely magmatic, resulting in a higher eruption column, up to 13 km. This phase of the eruption produced an upper lenticular layer of coarse tephra and bombs of scoriaceous basaltic andesite (the Plinian phase after (Degterev and Chibisova, 2019), from 22:30 to 2:00 UTC June 21–22, 2019).

The termination of violent explosive activity was followed during a few days by low-level, probably phreatomagmatic, activity in the crater discharging small clouds of fine ash (see Fig. 3a). Mostly phreatomagmatic mechanism of the eruption is inferred from the following facts: fine-grained grain size of discharged pyroclastic material, relatively low temperature and low gas content of the pyroclastic flow deposits, high content of non-juvenile rock fragments in the deposits and the comparatively low degree of vesicularity of the juvenile material.

**The morphologic changes in the island resulting from the eruption.** A study of satellite images detected that the main part of hot pyroclastic material was mostly deposited on the slopes of the northeastern sector of the volcano (Fig. 7a). A layer of pyroclastic material about 1 m thick was deposited on the western coast of the island (see Fig. 3c). The lower slopes and the base of the volcano were covered by a sequence of hot pyroclastic flow deposits which were steaming during the first few months after the eruption (see Figs. 3c, 8a).

A new shoreline was formed in the west, north, and northeast of the island 100–250 m farther seaward; its length was about 5 km (see Figs. 3b, 7a). The shoreline remained nearly the same in the southeastern sector

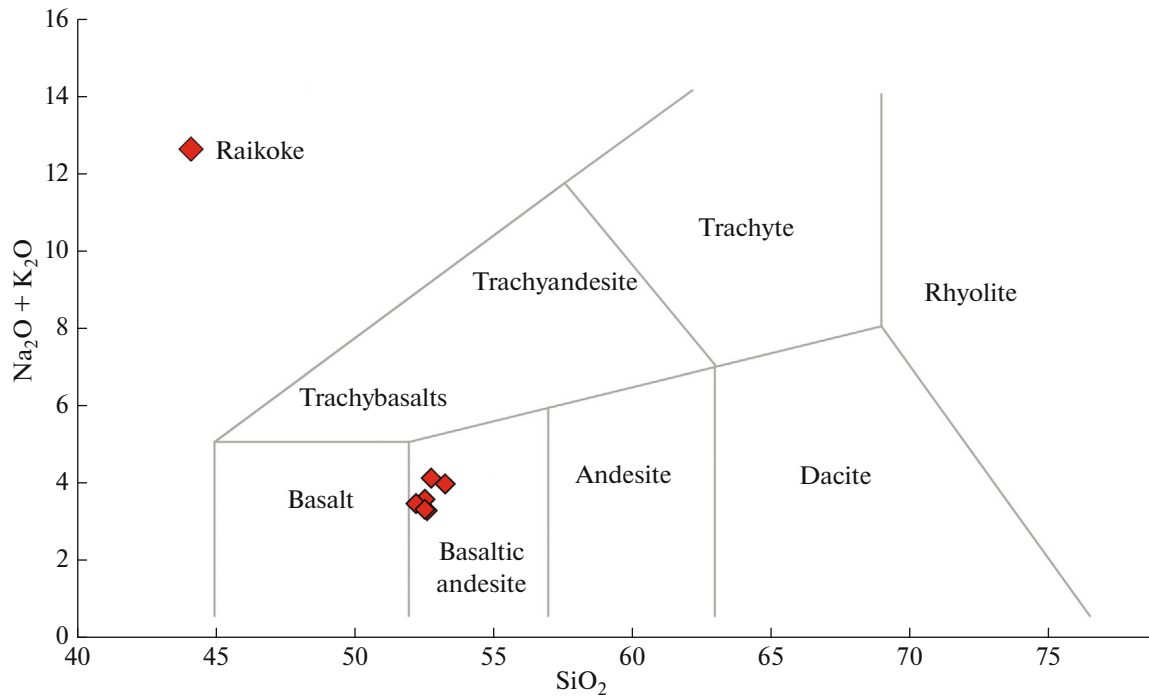


**Fig. 6.** The chemical composition of juvenile material of the 2019 eruption of Raikoke volcano. The compositions and names of rock types according to (Bas et al., 1986).

for a distance of about 900 m. Other coastal areas had some individual fans of pyroclastic material extending into the sea. The largest pyroclastic fan, located on the southwestern coast, in July 2019 it was ~480 m long and ~70 m high and extended to the sea up to 250 m (see Fig. 3c).

The overall area of the island increased after the eruption by 0.57 km<sup>2</sup> based on a satellite image taken on September 29, 2019 (see Fig. 7b), but immediately after the eruption the increase seems to have been slightly larger, about 0.7 km<sup>2</sup>. These estimates are close to the values reported by Romanyuk and Degtrev (2020). The volume of new pyroclastic material on the island (without distant tephra fallout) can be estimated 0.05 km<sup>3</sup>. Firstov et al. (2020) studied the acoustic signals generated by the 2019 eruption to estimate the total

volume of the pyroclastic material ejected by this eruption as 0.1 km<sup>3</sup>, and its explosivity as 4 on the VEI scale (Newhall and Self, 1982).

**The transformations of the environment during the first post-eruption year.** During the first year the intensive erosion and redeposition of pyroclastic material along the island’s shoreline, mostly from west to east, along the northern and southwestern coasts took place. Currents of sediment-laden water could be seen in satellite images at distances over 1 km south-east of the island.

As a result of erosion and redeposition the beaches on the western and northern coasts were reduced in size and became narrow (see Fig. 7), while the outcrops of fresh pyroclastic material on the island’s northern coast were 20–25 m high in 3 months after

**Table 1.** The chemical composition of juvenile material ejected by Raikoke Volcano during the 2019 eruption

| Sample | SiO <sub>2</sub> , % | Al <sub>2</sub> O <sub>3</sub> , % | Fe <sub>2</sub> O <sub>3</sub> , % | MnO, % | MgO, % | CaO, % | Na <sub>2</sub> O, % | K <sub>2</sub> O, % | TiO <sub>2</sub> , % | P <sub>2</sub> O <sub>5</sub> , % | Total |
|--------|----------------------|------------------------------------|------------------------------------|--------|--------|--------|----------------------|---------------------|----------------------|-----------------------------------|-------|
| R-3-6  | 52.79                | 17.58                              | 8.87                               | 0.171  | 4.44   | 9.37   | 2.99                 | 1.09                | 0.698                | 0.17                              | 98.51 |
| R3-7a  | 52.64                | 16.8                               | 8.89                               | 0.169  | 6.53   | 11.06  | 2.38                 | 0.86                | 0.645                | 0.13                              | 100.5 |
| R-5-1  | 53.29                | 18.39                              | 8.84                               | 0.169  | 4.79   | 10.33  | 2.9                  | 1.03                | 0.697                | 0.17                              | 100.5 |
| R-6    | 52.56                | 16.61                              | 9.61                               | 0.173  | 6.52   | 10.27  | 2.63                 | 0.9                 | 0.672                | 0.14                              | 100   |
| R-NN1  | 52.24                | 16.67                              | 9.66                               | 0.177  | 6.69   | 10.55  | 2.55                 | 0.87                | 0.703                | 0.13                              | 100.6 |
| R-NN2  | 52.56                | 16.18                              | 9.31                               | 0.174  | 6.84   | 10.8   | 2.42                 | 0.85                | 0.655                | 0.12                              | 100.3 |

Samples R-3-6 and R3-7a of pyroclastic flows, R-5-1 and R-6 of bombs, R-NN1 and R-NN2 of light grey pumiceous and grey scoriaeous material sampled by N.N. Pavlov on June 22, 2019.

the eruption (see Fig. 8c). The lava capes on the northwestern part of the island (see Fig. 1b), which were completely buried by deposits of pyroclastic flows during the eruption (see Figs. 7a, 7b), afterwards gradually became exposed again during the first post-eruption year (see Fig. 7e). The extensive fans of pyroclastic flows were completely eroded away and disappeared. As an example, the fan on the southwestern coast, which extended into the sea for a distance of ~250 m in July 2019 (see Figs. 3c, 7b), had been completely eroded away during time period of 5 months (see Fig. 7c). Pyroclastic material that was redeposited in spring–summer 2020 in this location formed a new beach about 1000 m long and up to about 250 m wide (see Figs. 7e, 7f). The small bays between the lava capes on the eastern side of the island (see Fig. 1b) were filled with redeposited pyroclastic material; the coastline with a large lava cape protruding for 250 m before the eruption was smoothed out, became less sinuous, and even linear in places (see Figs. 7d–7f).

Pyroclastic deposits on the coast cooled during six months after the eruption, and snow pack was seen on the island during the winter of 2019–2020 (images taken on December 20, 2019 (see Fig. 7c), on March 26, 2020 and April 5, 2020). However, the image of February 2, 2020 (see Fig. 7d) showed the island surface to be white-brown, the same as in the summer of 2019. Thus Raikoke may have experienced a single weak ash deposition of small phreatic explosion in the winter of 2019–2020 due to interaction between water and still hot pyroclastic deposits, or alternatively as a result of large collapse in the crater, producing a dust cloud. In a month after the eruption, a lake appeared in the crater due to percolating seawater (Melnikov et al., 2020). It is clearly visible in the satellite image of August 2, 2020 (see Fig. 7e).

**The impact on the ecosystems.** The upper and middle slopes of Raikoke had the mechanical and thermal impact due to flows of pyroclastic material. The existing soil and vegetation was largely torn away and buried. The least affected areas were the lower slopes in the southern half of the island. Comparison of ground-based photographic images (including a survey made from a drone) in 2019 and in 2020, showed that the patches of vegetation were preserved on the lower slopes and on bedrock pedestals where it covered only 5–10% in some areas (see Figs. 8d, 8e). This was clearly visible in the eastern and southern half of the island; as an example, patches of persistent vegetation were visible on the southern slope up to a height of 350 m a.s.l.; these patches were at a distance of about 340 m from the crater rim (see Fig. 3b). A large area of vegetation was preserved (although considerably distorted) at a distance of 200 m from the former coastline (see Fig. 8d). Overall, the cover of surviving vegetation is less than 1% on the island. The surviving plants are mostly the grass *Leymus mollis* (see Fig. 8e). The eruption also impacted the algae thickets along the coast of island: the algae were buried by pyroclastic

material emplaced in the sea (see Fig. 8f) and only some algae survived at the distances from the shore.

The rookery of Steller sea lions on the western coast was buried under deposits of hot pyroclastic flows. On July 12 and September 8, 2019, there were only 35 surviving animals, males on the opposite side of the island (Burkanov et al., 2020). The surveys made in a year after the eruption revealed 164 (June 18, 2020) and 174 (July 12, 2020) animals, including puppies (Burkanov et al., 2021). Thus the 2019 eruption caused a dramatic decrease in the population of sea lions on the island.

## DISCUSSION

The volume of the material erupted by the 2019 eruption and deposited on the island, and forming a new land, as well as emplaced under water in the sea, near the island, comprises about 0.05 km<sup>3</sup>, with the addition of distal tephra, it would comprise about 0.1 km<sup>3</sup>. Basing on the erupting volume and on a maximum height of the eruption column (13 km), the eruption had violence 4 on the VEI scale (Degterev and Chibisova, 2019), that indicates that 2019 eruption violence similar to the 1778 and 1924 eruptions, which were also classified as VEI 4 (Siebert et al., 2011). Similarly to the past historical eruptions, the 2019 eruption started suddenly and was characterized by high explosivity, which was due to the phreatomagmatic character of fragmentation affecting the rising magma that contacted ground water. Probably the ground water was represented by seawater percolating into the edifice of the volcano from outside. This hypothesis is based on the fact that after the 2019 eruption the seawater rapidly percolated into the deepened crater, making a crater lake (Melnikov et al., 2020). Such mechanism is typical for explosive eruptions of Raikoke and is likely to repeat in the future. However, the volcanic cone of Raikoke is composed mostly of of “aa” lava flows, which probably erupted in times, when the access/inflow of ground water (including sea water) to the Raikoke magmatic conduit was limited. In the future Raikoke may revert to the dominantly effusive style of activity in case the hydrogeological situation inside its edifice will change.

One special feature of Raikoke Island is its small dimensions (the coast is a mere 0.4–1 km from the crater); consequently, all of its area is severely affected by the volcanic eruptions. The slopes are steep, resulting in pyroclastic flows propagating toward the base of the volcano, where they enter the sea and create a new coastline, which is then gradually, but rapidly enough, eroded by the sea.

One of the first publications devoted to this eruption (Girina et al., 2019) presented a description of white steam plumes that were visible in some satellite images, hypothesizing that a lava flow was extruded onto the slope of the volcano and that submarine vol-

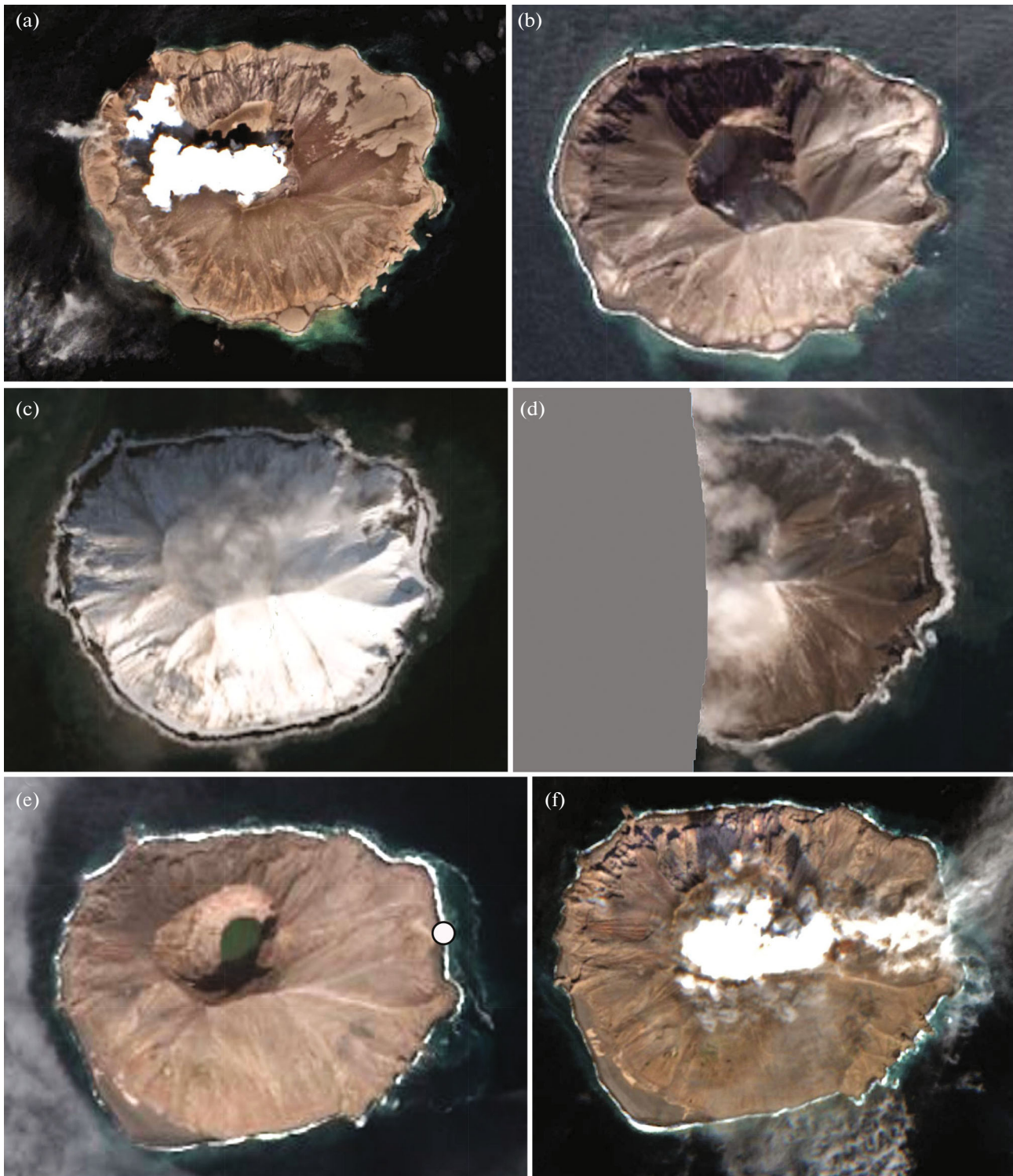


**Fig. 7.** Satellite images showing changes of deposits in the coastal area of Raikoke during one year since the 2019 eruption: June 30, 2019 (a), September 29, 2019 (b), December 20, 2019 (c), February 2, 2020 (d), August 2, 2020; the white dot marks the site of of detailed onland investigations in July 2020 (e), in September 2, 2020 (f). Images 7a–7f are from the Sentinel 2 satellite, 7b–7e are from WorldView-2. The missing parts of the image in Fig. 7d were lost due to the technical problems of satellite. Diameter of the island (2 km) gives a scale.



**Fig. 8.** The lava cape in the western coast of the island Raikoke on June 23, 2019 (a) and in July 2020 (b); part of the Raikoke northern coast in July 2020 (c); areas of fragmentary surviving vegetation at the base of slopes on the eastern coast, July 2020 (d); an area with surviving beds of grasses and new birds' nests on the eastern coast of the island, July 2020 (e); algae partly buried by pyroclastic material, June 23, 2019 (f). Photographed by N.N. Pavlov (a, b, d, f), by O.A. Rumyantseva (c), and by A.B. Belousov (e).

cano 3.18 was simultaneously erupting 6.5 km northwest of Raikoke (Rashidov et al., 2006). Our 2020 field surveys on the islands did not detect any signs of fresh lava flows and signs of a submarine eruption. This interpretation of white steam plumes was probably erroneous, the plumes being caused by pyroclastic flows from Raikoke entering the sea.

Special feature of the island is a constant abundant supply of organic matter in its ecosystem (fish—sea birds—bird droppings—soil—vegetation), which considerably accelerates succession at volcanogenic deposits. In addition, by building the nests in an unconsolidated pyroclastic substratum, birds produce microrelief inhomogeneities (see Fig. 8e), which favors vegetation settlement. The succession is also accelerated by small episodic ashfalls from adjacent volcanoes of the Kuril

island arc. For example, the ashfall on Raikoke from erupting Sarychev Peak Volcano (Matua Island) in June 2009 (personal communication of observer V.V. Chernitsyn who was on duty on Raikoke).

The transformation cycle for the Raikoke environment was probably similar to the processes that occurred on Matua Island after a strong eruption of Sarychev Peak Volcano in 2009 (Grishin, 2011). Being part of the Kuril island arc, both of these islands are 16 km apart (see Fig. 1) and are characterized by similar natural conditions. However, the increasing of island area after the eruption on Matua was 2–3% of island area, while on Raikoke was ~15%. On Matua the thick pyroclastic deposits settled down in the sea led to the formation of new land and produced a scalloped coastline; subsequently, the new coastline was

smoothed out (during the first few months), the deposits were eroded away and transported from west to east into neighboring bays (during the first few years). Looking at the slopes of Sarychev Peak over which hot flows of pyroclastic surges passed, we find that the lifelessness of the first year after the eruption gradually gave way to recovery of a small part of surviving (though damaged) vegetation, mostly grasses. Pioneering plants settled down on primary substrata. The algae thickets also recovered rapidly enough (during a single decade) in the coastal zone of Matua Island.

Similar processes with some modifications occur on Raikoke now. The recovery of the Raikoke ecosystems is connected with the erosion of volcanic deposits, gradual settlement of birds on the new substratum (this was recorded as early as in September 2019) with accompanying supply of new plant species to the island. A considerable impulse to succession is expected to come from fragmentary patches of survived vegetation (including that which is partly buried). Primary succession will occur in stages with the dominant kind being mosses to pioneering herbs and tiny bushes to herbaceous plants and bushes to creeping woody vegetation. The final stage will produce a continuous cover consisting of grasses and creeping vegetation.

The period of complete recovery must last at least ~200 years as we estimate for the conditions prevailing on Raikoke, but the recovery is constantly interrupted by periodic large eruptions during middle stages of recovery. Thus, the nature of this volcanic island typically involves periodic catastrophic destructions of the ecosystems during large explosive eruptions and comparatively rapid recovery processes to be interrupted by a next eruption.

#### ACKNOWLEDGMENTS

We wish to thank for the photographs and videos of Raikoke Island, as well as for the observations, the following persons: N.N. Pavlov, V.Yu. Barkalov, E.V. Kaspersky, O.A. Rumyantseva, A.M. Trukhin, and V.V. Chernitsyn. Special thanks go to E.G. Kalacheva who organized operations on Raikoke in 2016 and in 2020, and to the crews of the vessels *Afina* (2016) and *Ashura* (2020) for the trip to the island. We thank the reviewers whose remarks helped to improve the manuscript.

#### FUNDING

The work on Raikoke Island was done in 2016 and in 2020 for the projects supported by the Russian Science Foundation, nos. 15-17-200011 and 20-17-00016.

#### REFERENCES

- Bas, M.L., Maitre, R.L., Streckeisen, A. et al., A chemical classification of volcanic rocks based on the total alkali-silica diagram, *J. of Petrology*, 1986, vol. 27, no. 3, pp. 745–750.
- Burkanov, V., Gurarie, E., Altukhov, A., et al., Environmental and biological factors influencing maternal attendance patterns of Steller sea lions (*Eumetopias jubatus*) in Russia, *J. of Mammalogy*, 2011, vol. 92(2), pp. 352–366.
- Burkanov, V., Pavlov, N., and Gelatt, T., Catastrophic destruction of Raykoke Island Steller sea lion rookery by volcanic eruption: June, 2019, *Abstracts of Alaska Marine Science Symposium*, Anchorage, Alaska, 2020, p. 216.
- Burkanov, V., Russel, A., and Gelatt, T., One year later: Modest recovery of the Raykoke Island Steller sea lion rookery after the June 2019 volcanic eruption, *Alaska Marine Science Symposium*, 2021, p. 144.
- Degterev, A.V. and Chibisova, M.V., The June 2019 eruption of Raikoke Volcano, Raikoke Islands, Central Kuril Islands, *Geosistemy Perekhodnykh Zon*, 2019, issue 3, no. 3, pp. 304–309.
- Firstov, P.P., Popov, O.E., Lobacheva, M.A., et al., Wave disturbances in the atmosphere that accompanied the June 21–22, 2019 eruption on Raikoke Volcano, Kuril Islands, *Geosistemy Perekhodnykh Zon*, 2020, vol. 4, no. 1, pp. 71–81.
- Girina, O.A., Loupyan, E.A., Uvarov, I.A., et al., The June 21, 2019 eruption of Raikoke Volcano, *Sovr. Probl. Dist. Zond. Zemli Kosm.*, 2019, no. 16(3), pp. 303–307.
- Gorshkov, G.S., A chronology of volcanic eruptions at the Kuril island arc (1713–1952), *Trudy Labor. Vulkanol. AN SSSR*, 1954, no. 8, pp. 58–99.
- Gorshkov, G.S., The active volcanoes of the Kuril island arc, *Tr. Labor. Vulkanol.*, 1958, no. 13, pp. 5–70.
- Gorshkov, G.S., *Vulkanizm Kuril'skoi ostrovnnoi dugi* (The Volcanism of the Kuril Island Arc), Moscow: Nauka, 1967.
- Grishin, S.Yu., The environmental impact of the powerful eruption of Saryshev Pik Volcano, Kuril Islands, 2009, as reported by surveys from space, *Issl. Zemli Iz Kosmosa*, 2011, no. 2, pp. 92–96.
- Hoblitt, R.P. and Harmon, R.S., Bimodal density distribution of cryptodome dacite from the 1980 eruption of Mount St. Helens, Washington, *Bull. Volcanol.*, 1993, vol. 55(6), pp. 421–437.
- Houghton, B.F. and Wilson, C.J.N., A vesicularity index for pyroclastic deposits, *Bull. Volcanol.*, 1989, vol. 51(6), pp. 451–462.
- Inman, D.L., Measures for describing the size distribution of sediments, *J. of Sedimentary Research*, 1952, vol. 22(3), pp. 125–145.
- Markhinin, E.K. and Stratula, D.S., Some new evidence on the volcanism of the Kuril Islands, in *Chetvertichnyi vulkanizm nekotorykh raionov SSSR (The Quaternary Volcanism in Some Areas of the USSR)*, Moscow: Nauka, 1965, pp. 14–28.
- Melnikov, D.V., Ushakov, S.V., Girina, O.A., et al., The formation of new lakes in the active crater of Mutnovsky Volcano and in the crater of Raikoke Volcano, in *Materialy nauchnoi konferentsii, posvyashchennoi Dnyu vulkanologa* (Proc. of the conference devoted to Volcanologist's Day), Petropavlovsk-Kamchatsky: IViS DVO RAN, 2020, pp. 42–44.
- Newhall, C.G. and Self, S., The Volcanic explosivity index (VEI): An estimate of explosive magnitude for histori-

- cal volcanism, *J. Geophys. Res.*, 1982, vol. 87, pp. 231–238.
- Plechov, P.Yu., Shishkina, T.A., Ermakov, V.A., and Portnyagin, M.V., The conditions that prevailed during the generation of allivalites (olivine–anorthite crystalline inclusions) in volcanic rocks of the Kuril–Kamchatka island arc, *Petrologiya*, 2008, vol. 16, no. 3, pp. 1–30.
- Polonsky, A., The Kuriles, in *Zapiski Imperatorskogo Russkogo Geograficheskogo Obshchestva po Otdeleniyu Et-nografii* (Proceedings of the Russian Emperor Geographic Society for the Ethnographic Section), St. Petersburg: Tipografiya Maikova, 1871, vol. 4, pp. 367–576.
- Rashidov, V.A., Bondarenko, V.I., Romanova, I.M., et al., Geophysical surveys of underwater volcanoes at the Kuril island arc in electronic information resources at the Internet, in *Materialy nauchno-tehnicheskoi konferentsii “Geofizicheskii monitoring Kamchatki”* (Proc. conference “Geophysical Monitoring of Kamchatka”), Petropavlovsk-Kamchatsky: IViS DVO RAN, 2006, pp. 75–82.
- Rashidov, V.A., Girina, O.A., Ozerov, A.Yu., et al., The June 2019 eruption of Raikoke Volcano, Kuril islands, *Vestnik KRAUNTs, Nauki o Zemle*, 2019, no. 2, issue 42, pp. 5–8.
- Romanyuk, F.A. and Degterev, A.V., The change in shore-line configuration of Raikoke Island after the explosive eruption of June 21–25, 2019, Central Kuril Islands, *Geosistemy Perekhodnykh Zon*, 2020, issue 4, no. 3, pp. 351–358.
- Siebert, L., Simkin, T., and Kimberly, P., *Volcanoes of the World*, Third Edition, California: University of California Press, 2011.
- Takahashi, H., Barkalov, V.Y., Gage, S., et al., A floristic study of the vascular plants of Raikoke, Kuril Islands, *Acta Phytotax. Geobotanica*, 2002, vol. 53(1), pp. 17–33.
- Tanakadate, H., Volcanic activity in Japan and vicinity during the period between 1924 and 1931, *Japanese Journal of Astronomy and Geophysics*, 1931, vol. 9, p. 47.
- Truhin, A.M., Raikoke Island and its inhabitants, *Priroda*, 2008, no. 6, pp. 33–42.
- Walker, G.P., Grain-size characteristics of pyroclastic deposits, *J. of Geology*, 1971, vol. 79(6), pp. 696–714.

*Translated by A. Petrosyan*